Journal of Crystal Growth 312 (2010) 1122–1126

Contents lists available at ScienceDirect

Journal of Crystal Growth

journal homepage: www.elsevier.com/locate/jcrysgro

Growth and defect structure of $ZnGeP_2$ crystals

G.A. Verozubova [a,*], A.O. Okunev [b], A.I. Gribenyukov [a], A.Yu. Trofimiv [a], E.M. Trukhanov [c], A.V. Kolesnikov [c]

[a] Institute of Monitoring of Climatic and Ecological Systems SB RAS, Tomsk, Russia
[b] Yaroslav-the-Wise Novgorod State University, Veliky Novgorod, Russia
[c] Institute of Physics of Semiconductors SB RAS, Novosibirsk, Russia

ARTICLE INFO

Available online 10 November 2009

Keywords:
A1. Defects
A1. Crystal structure
A2. Growth from melt
B1. Phosphides
B2. Nonlinear optical materials
B2. Semiconducting ternary compounds

ABSTRACT

A defect structure of nonlinear optical material $ZnGeP_2$, grown by the vertical Bridgman technique from the melt, was studied. The state-of-the-art results in $ZnGeP_2$ growth with sufficiently perfect structure allow one to register the presence of Borrmann effect and to apply the X-ray topography method based on this effect for the first time. Microscopy and X-ray transmission topography based on the Borrmann effect revealed growth striation, precipitates, forming lineage structures along the growth axis, dislocations and unknown linear defects, which should be more elaborately studied in future. The observed defects are formed because of deviation from $ZnGeP_2$ stoichiometry during synthesis and growth and unfavorable thermal conditions during growth. The precipitates are observed only with significant deviations from stoichiometry. The width of rocking curves for the as-grown crystals is 13–35 seconds of arc, which shows a good structural perfection, in spite of the revealed defects. The thermal annealing and electron beam irradiation decrease the optical absorption coefficient at 2.06 μm to 0.02 cm^{-1}.

1. Introduction

Nonlinear optical materials are used in different applications of high-resolution spectroscopy, in particular, for remote monitoring of the atmosphere. Ternary compound $ZnGeP_2$ is a semiconductor with chalcopyrite structure from the II–IV–V_2 group. This compound has a unique set of optical and other properties (wide potential transmission range of 0.65–13 μm, a high second-order dielectric susceptibility d_{36}=75 pm/V, birefringence, sufficient for phase matching, high specific thermal conductivity, and high hardness) and is used as a high-performance nonlinear optical medium for laser radiation frequency conversion in the middle infra-red [1,2]. It is also a very promising material for creation of terahertz radiation sources [3,4].

Application of $ZnGeP_2$ in nonlinear optical devices demands from crystals a high structural perfection and uniformity of properties. However, a stable growth of perfect $ZnGeP_2$ crystals with high optical quality is a difficult scientific and technological problem. In particular, all the as-grown $ZnGeP_2$ crystals have a high optical absorption in the 0.65–2.5 μm region, which limits a wider application of these crystals in optical devices. It was revealed that a high concentration of vacancies of volatile components is responsible for this absorption [5–7].

The material has a rather high melting point, and a rather high pressure of vapor of volatile components (Zn and P) over its melt. The total pressure of saturated vapor over $ZnGeP_2$ in the melting point was determined to be equal to 3.5 [8] and 4.2 atm [9]. The partial pressures of Zn and P were not yet determined over $ZnGeP_2$. The literature shows different data for melting temperature of $ZnGeP_2$: 1020 °C [10], 1025 °C [11], 1027 °C [12], and 1038 °C [13]. Different data for melting point are apparently related to different compositions of the studied $ZnGeP_2$ samples because of the evaporation of the volatile Zn and P from the melt. Our past unpublished differential thermal analysis data showed that a value of $ZnGeP_2$ melting temperature is quite sensitive to the composition of the studied samples even through the vapor pressure, created by P and Zn amounts, added to the growth ampoule for compensating their evaporation from the melt during growth.

Presence of two readily volatile components (Zn and P) that readily form binary compounds (ZnP_2 and Zn_3P_2) from vapor phase and absence of reliable data on *P–T–x* diagram near the ternary $ZnGeP_2$ compound leads to deviation from stoichiometry of melt composition during synthesis and growth. The latter is the most probable reason for emergence of high concentration of point defects, and is responsible for high absorption in the near-IR region of $ZnGeP_2$ transparency range. These deviations may also

* Corresponding author. Tel.: +7 3822 492589; fax: +7 3822 491950.
E-mail address: verozubova@mail.tomsknet.ru (G.A. Verozubova).

0022-0248/$ - see front matter © 2009 Elsevier B.V. All rights reserved.
doi:10.1016/j.jcrysgro.2009.11.009

easily result in emergence of defects with higher dimension such as growth striae and precipitation of second phases and dislocations. However, these structural defects are less studied to date, and the mechanism of interaction of these defects with the point ones is not understood for $ZnGeP_2$. The main aim of this paper is to present our recent results on studies of defect structure of $ZnGeP_2$ crystals.

2. Experimental

To prepare $ZnGeP_2$ material from elements a two-temperature scheme of synthesis was used [14]. Phosphorus as the most volatile component was placed in the cold zone, while zinc and germanium were placed in the hot reaction zone. $ZnGeP_2$ was formed by reaction of the phosphorus vapor with condensed Zn and Ge in the hot reaction zone. The temperature conditions for reaction to form $ZnGeP_2$ are as follows: the cold zone temperature is 520 °C, which corresponds to the P vapor pressure of 10–11 atm, and the hot zone temperature is 1010 °C. To avoid transport of volatile binary zinc phosphides from reaction zone the cold zone temperature is increased after the reaction up to 1070 °C. Then the hot zone temperature is increased up to 1050 °C to melt and homogenize the synthesized compound. After 8 h of homogenization the material is slowly crystallized and cooled down. Such technology allows one to synthesize ~500 g of the material in one run.

For $ZnGeP_2$ single crystal growth Vertical Bridgman technique is used. The hot zone temperature is 1050–1060 °C and the cold zone temperature is 990–1010 °C. The temperature gradient near the melting point of $ZnGeP_2$ is 3–4 °C/cm. The solidification of $ZnGeP_2$ melt is realized by mechanical pulling of ampoule via the temperature gradient; a typical speed is about 1–0.5 mm/h. The single crystal nucleation is provided by means of seeds. Our past experiments show [15] that the most favorable crystallographic directions for $ZnGeP_2$ growth by VB are directions along the main chalcopyrite axes. In $ZnGeP_2$ crystals grown along other directions twins and cracks are observed. This is related to anisotropy of thermal expansion coefficients along the main axes of chalcopyrite lattice as shown by Feigelson and Route [16], by the example of $CdGeAs_2$. The grown single crystals are 20–30 mm in diameter and 100–170 mm in length. The yield of single crystals is about 80%.

To analyze the real structure of the as-grown $ZnGeP_2$, microscopy (optical transmission and scanning electron), X-ray transmission topography, based on the Borrmann effect [17], and rocking curves analysis were used. To obtain the X-ray topographs with the use of the Borrmann effect, the studied samples should be perfect enough (the dislocation density should be less than 10^3 cm^{-2}), and meet the condition $\mu_0 t \gg 1$, where μ_0 is a usual linear absorption coefficient (cm^{-1}) for X-rays and t is the thickness of the sample. For $ZnGeP_2$ the thickness should be 270 μm and more. For this study we used the samples of about 500 μm thickness. Also, measurement of optical transparency and calculation of optical absorption coefficient for as-grown, annealed, irradiated, and post-irradiated annealed $ZnGeP_2$ samples were performed.

3. Results and discussions

3.1. Growth striation

Fig. 1 demonstrates an optical transmission microscopy microphotograph of thin $ZnGeP_2$ slice (the thickness is less than 1 mm) cut along the growth axis. The growth axis is directed upwards. The growth striation is clearly seen here, it is dark and light striae. It is evident that such striation leads to oscillation of optical transparency along the growth axis. From the presented microphotograph it is seen that the striae have a concave shape. According to classification such striae are of the first type, since they are parallel to the growth interface, so a concave crystallization front is realized during growth. The second type of growth striae, which is not parallel to interface, was not revealed in $ZnGeP_2$. The most probable reason for growth striation in the Vertical Bridgman method is unsteady gravitational convection, arising from horizontal (radial) temperature gradient near the crystallization front [18]. The convection can be removed by providing a strictly axial heat flux, which corresponds to flat interface [16,18].

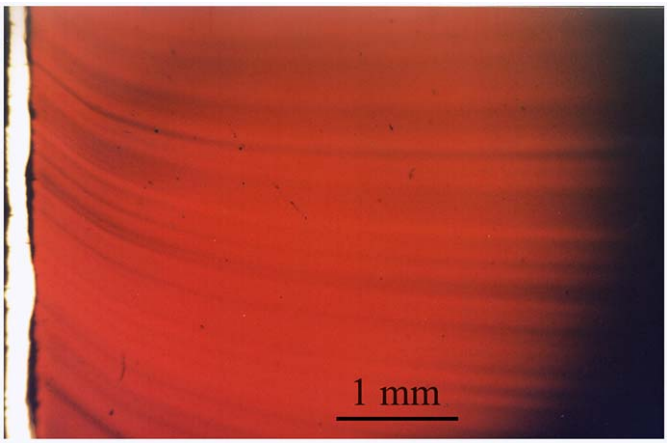

Fig. 1. Optical transmission microscopy microphotograph of thin $ZnGeP_2$ slice cut along the growth axis, demonstrating the growth striation. The growth axis is directed upwards.

Fig. 2a and b presents, correspondingly, a transmission microscopic image and X-ray topography image of the same $ZnGeP_2$ sample, cut along the growth axis. Both images visualize a growth striation in the sample. A character of the striae distribution is similar for optical and X-ray images: dark striae on microscopic image correspond to the dark striae on X-ray image as well as the light striae in microscopic image correspond to the light ones on topography image. It is very well seen with superposition of these images, shown in Fig. 2c. As shown in [19], the dark contrast on X-ray image corresponds to the lattice compression (lattice parameters are decreased), but light contrast corresponds to the lattice expansion (lattice parameters are increased). Dark contrast on microscopic image is stipulated by higher optical absorption. The contrast correlation can be apparently explained by the higher concentration of vacancies, which results simultaneously in lattice compression and increase of optical absorption in near IR. Thus, in our case the striation can be possibly related to oscillation of concentration of point defects of vacancy type. The X-ray topograph also demonstrates mixed dislocations, parallel to the growth axis.

3.2. Precipitates of second phases (solute trails)

Besides growth striae with significant deviations from stoichiometry the precipitates that form linear structures along the growth axis (so-called "solute trails") can be found in $ZnGeP_2$ crystals, grown by the Vertical Bridgman method. Fig. 3a and b presents correspondingly optical transmission image and electron scanning image of "solute trails". As a rule the "solute trails" are located in the center of the crystal cross-section, near the crystal

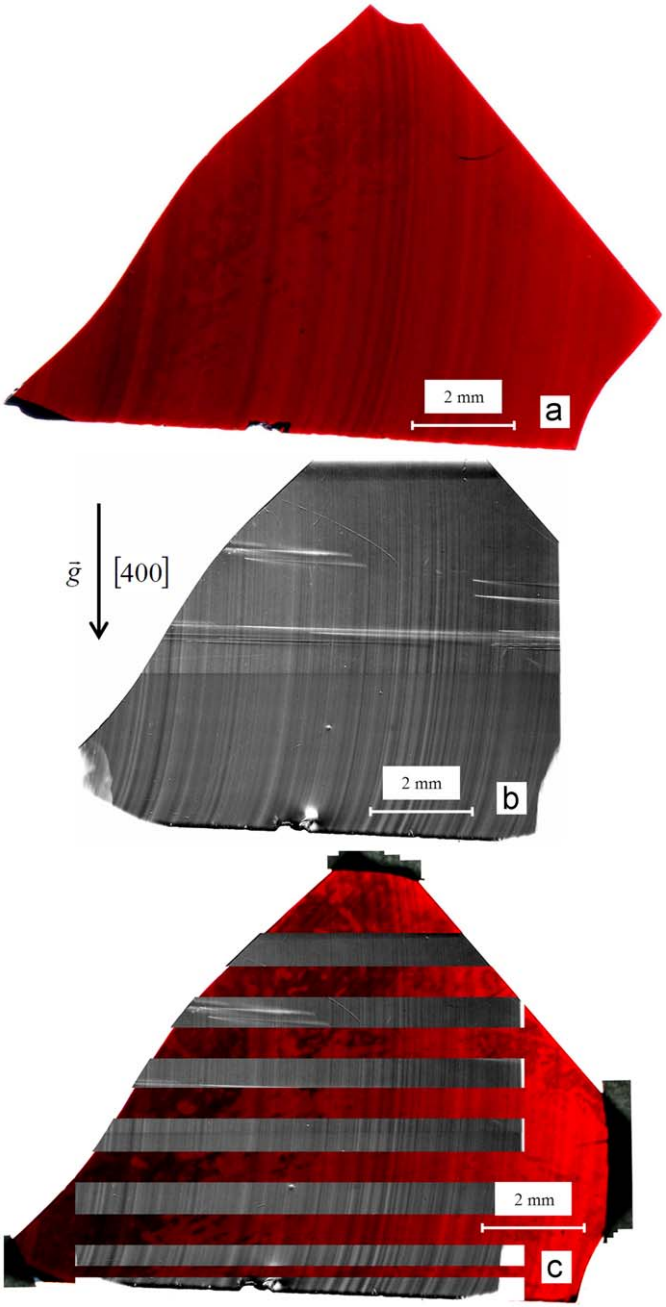

Fig. 2. (a) Microscopy image and (b) X-ray transmission topography image of the same $ZnGeP_2$ thin sample. (c) superposition of these images.

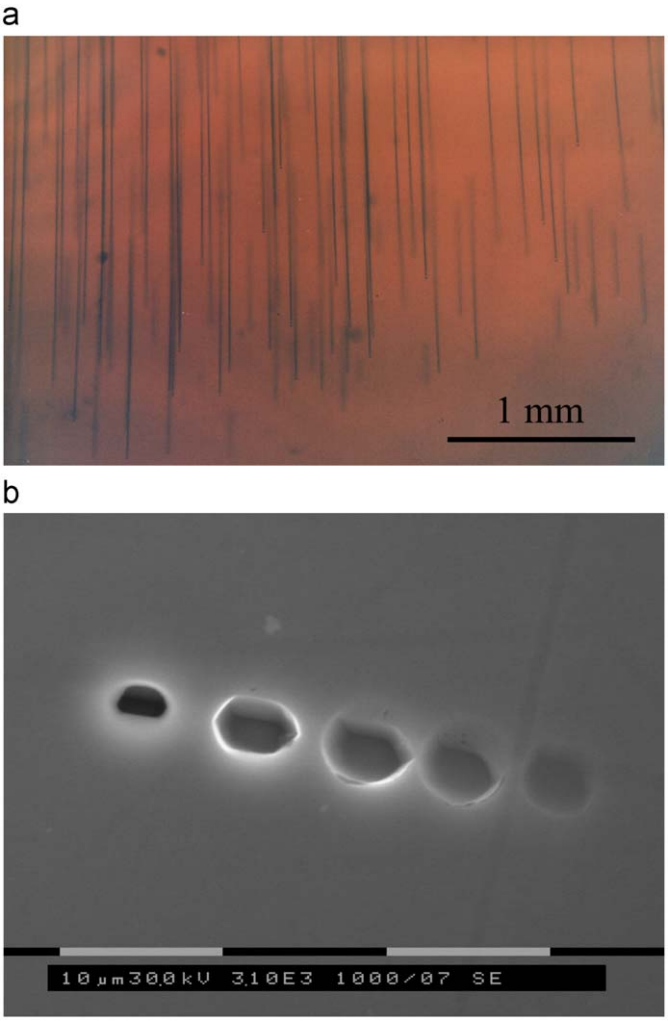

Fig. 3. (a) Optical transmission image of precipitates in solute trails and (b) its corresponding electron scanning image.

axis. Such location is stipulated by concavity of the crystallization front during $ZnGeP_2$ growth [20].

Fig. 4 presents X-ray transmission topograph with the "solute trails". Fig. 4b is an enlarged image of the fragment outlined by rectangular frame on the topograph shown in Fig. 4a. As seen from the presented X-ray topograph the precipitates in "solute trails" generate dislocations with a big edge component of Burgers vector. The dislocations are born on precipitates forming the "solute trails". The sharp end of dislocation images corresponds to exit of dislocation on the sample surface; the washed tails are created by deep part of the dislocation line. The dislocation image is widened because of the impurity atmospheres, associated with the dislocations. Such dislocations, born on "solute trails", can be responsible for crack formation in $ZnGeP_2$ crystals.

It is evident that the presence of "solute trails" may significantly increase the optical losses in $ZnGeP_2$: the higher density of the "solute trails" gives the higher optical losses. For example, for the same as-grown sample the optical transparency, measured at 5 μm, where the absorption, caused by point defects, is practically absent, was 54% (because of the high value of refractive indices the maximum transparency in $ZnGeP_2$ is 56%) with zero density of solute trails, 49% with density of "solute trails", equal to 1200 cm^{-2}, and 20% with the density, equal to 4500 cm^{-2}. These optical losses are stipulated not only by scattering of light but also by "shadow" effect, when a part of the sample with "solute trails" is not transparent for the light.

Fig. 5 demonstrates a topograph of the central part of cross sample of $ZnGeP_2$, cut perpendicular to growth axis $<0\,0\,1>$. The topograph was obtained with the use of strongly asymmetrical reflection $[\bar{2}02]$. As seen from the topograph, a part of the defects, located in the crystal volume, organizes images in the form of wide diffusion tails. At the intersection of the defects of the crystal surface, which is the outflow face for X-rays, "rosettes" of contrast, typical for inclusions, are fixed. When the defect line coincides with the direction of primary propagation of energy in crystal, the contrast is formed as a result of complete lack of anomalous transmission in the crystal column containing the defect. It is possible that these defects may present some initial stage of solute trails nucleation. Meanwhile, under optical

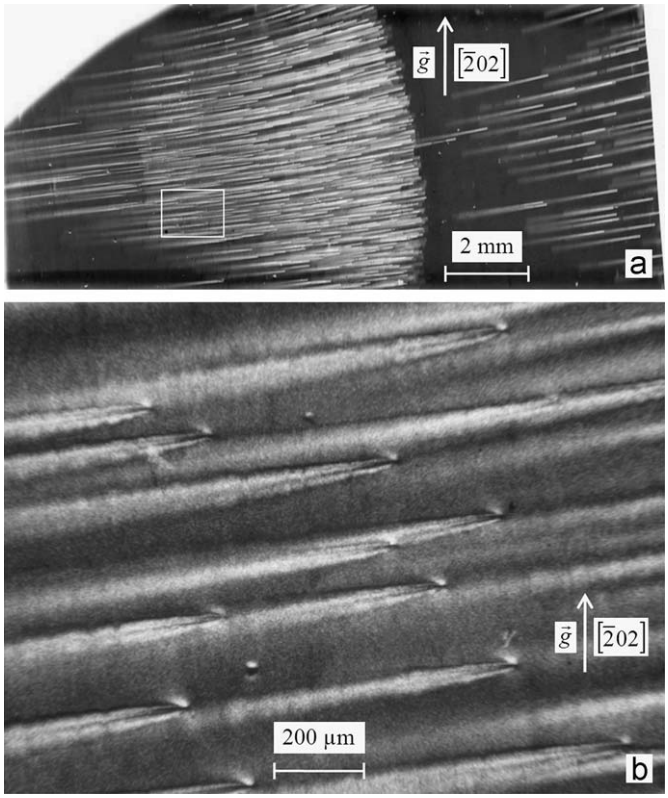

Fig. 4. (a) A general X-ray transmission topograph of the sample with solute trails and (b) enlarged fragment of the topograph outlined by frame in (a).

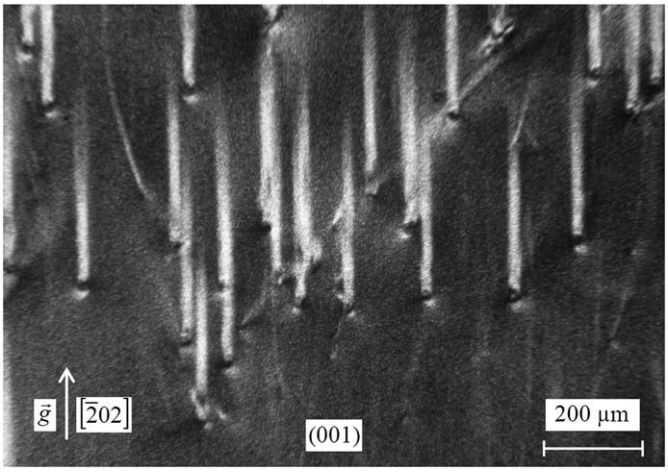

Fig. 5. X-ray transmission topograph of central part of the cross sample of $ZnGeP_2$, cut perpendicular to the growth axis ⟨0 0 1⟩.

microscopy examination there is no evidence of "solute trails" and further study is needed to elucidate the nature of these defects.

3.3. Rocking curves analysis

A typical width of the rocking curves for the as-grown $ZnGeP_2$ crystals is about 15–35 seconds of arc, which is an evidence of their high structural perfection. However, it was revealed that the width of the rocking curves is larger for the central parts of the ingot than that for the peripheral parts, which is probably related to accumulation of point and other defects near the growth axis of the ingot because of the concave crystallization front. Note that the studied samples do not contain the solute trails. Corresponding rocking curves and calculated width of the rocking curves for central and peripheral parts of 3 cross slices, cut from the onset, middle, and end of one single crystal ingot, are shown in Fig. 6.

3.4. Optical absorption

Optical absorption study of $ZnGeP_2$ crystals was carried out on samples that did not contain "solute trails". All other revealed defects described above might be present. Their influence on optical transparency of $ZnGeP_2$ crystals is not recognized yet.

In the wavelength range 2.5–8 μm, $ZnGeP_2$ crystals generally have a high transparency (~56%); therefore, we do not show this part of the spectrum. Fig. 7 shows the typical optical absorption coefficient spectra of $ZnGeP_2$ single crystal in the optical range 0.75–2.6 μm. In the as-grown state (curve 1 in Fig. 7), the typical value of the optical absorption coefficient at a wavelength of 2.06 μm is about 0.3–0.5 cm^{-1}; this high value does not allow one to use the $ZnGeP_2$ crystals in OPO devices with pumping near 2.06 μm. The absorption at this wavelength can be significantly reduced by thermal annealing and high-energy electron irradiation. For example, after thermal annealing of $ZnGeP_2$ crystals at 600 °C during 400 h in vacuum, the absorption coefficient at a wavelength of 2.06 μm can be decreased down to 0.1–0.2 cm^{-1} (Fig. 7, curve 2). The best samples after thermal annealing can have the absorption coefficient equal to ~0.08–0.07 cm^{-1} at wavelength 2.06 μm. Further, in-depth improvement of optical transparency at this wavelength may be attained by electron beam irradiation, as shown in Fig. 7, curve 3. After being annealed and irradiated by electrons with 4 MeV energy, the $ZnGeP_2$ crystals can have an absorption coefficient not larger than ~0.02 cm^{-1}.

Fig. 8 shows changes in the optical absorption coefficient with low-temperature annealing of one $ZnGeP_2$ sample after its irradiation by high electron fluence (dose) 2.9×10^{17} cm^{-2}. As seen from the figure these changes have already begun with 160 °C, but the annealing mainly affects only on absorption in the 0.7–1.3 μm part of the spectrum up to temperatures ~320 °C. The optical absorption in the spectral range ~1.3–2.5 μm has very little changes at these temperatures (160–320 °C), so the absorption coefficient is practically stable at 2.06 μm after irradiation under low-temperature annealing. Considerable

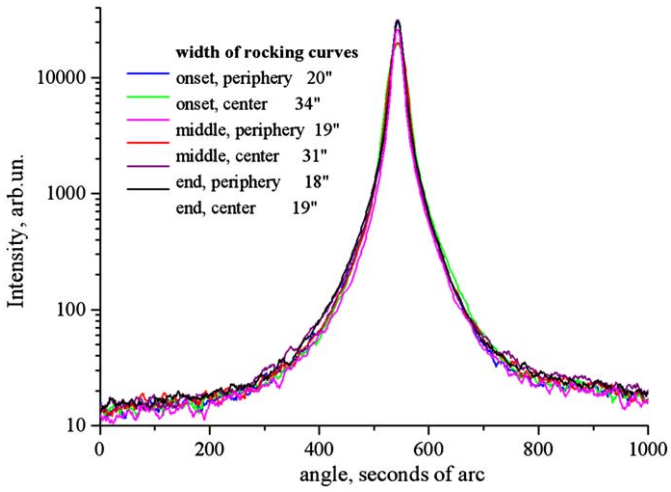

Fig. 6. Rocking curves and calculated width of the rocking curves for central and peripheral parts of 3 cross slices, cut perpendicular to growth axis <0 0 1> from the onset, middle, and end of one single crystal as-grown $ZnGeP_2$ ingot.

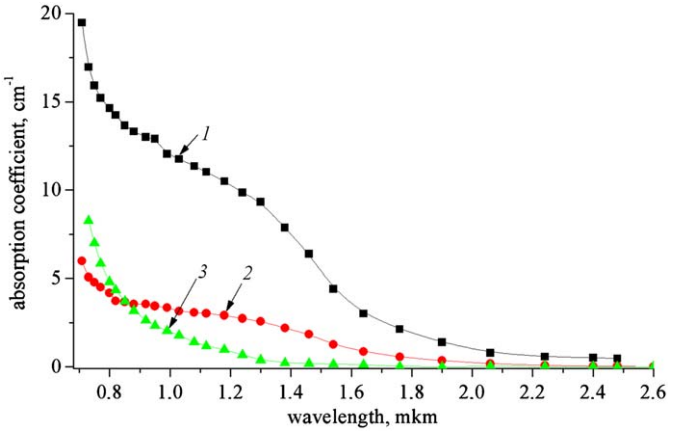

Fig. 7. Optical absorption coefficient spectra (o-ray) for $ZnGeP_2$: 1—as-grown sample, 2—annealed sample, and 3—irradiated sample (fluence 1.5×10^{17} cm^{-2}).

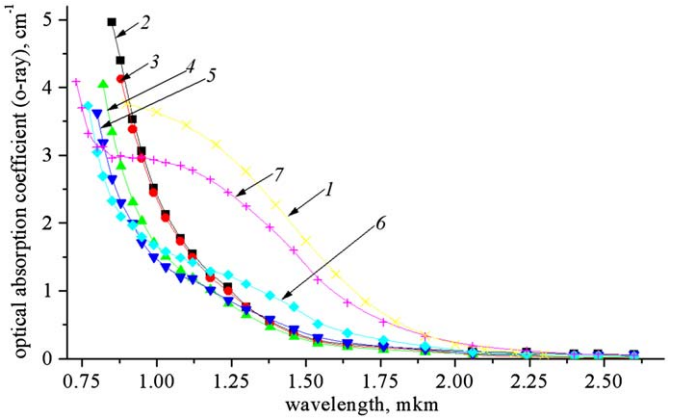

Fig. 8. Optical absorption coefficient spectra (o-ray) for one $ZnGeP_2$ sample: as-annealed state (curve 1), irradiated state (curve 2, fluence 2.9×10^{17} cm^{-2}), and then annealed after irradiation at different temperatures during 20 min: 3 at 160 °C, 4 at 260 °C, 5 at 320 °C, 6 at 400 °C, and 7 at 520 °C.

changes of absorption in the ~1.3–2.5 μm part of spectrum of irradiated samples (their return to as-annealed state) begin at temperatures 400–520 °C, as shown in Fig. 8.

4. Conclusions

A highly productive technology of $ZnGeP_2$ synthesis from the elements and $ZnGeP_2$ single crystal growth by the Vertical Bridgman method were developed. Thermal annealing and electron irradiation allow decreasing the optical absorption coefficient in $ZnGeP_2$ at the wavelength 2.06 μm down to ~0.02 cm^{-1}, which allows one to use $ZnGeP_2$ crystals efficiently as OPO with pumping near 2 μm.

However, a number of structural defects have been revealed in $ZnGeP_2$ crystals at the same time.

Optical transmission and scanning electron microscopy and rocking curves analysis have been carried out for the as-grown crystals. Effect of anomalous transmission of X-rays has been revealed in $ZnGeP_2$ crystals and the method of X-ray topography based on the Borrmann effect has been realized to study the structure of the crystals. The applied methods revealed the following structural defects in $ZnGeP_2$ crystals as-grown by the Vertical Bridgman method: growth striae, inclusions of second phases, forming lineage structure of precipitates (solute trails), and dislocations as well. Besides, X-ray topography also reveals the linear defects near the crystal axis, which cannot be identified as inclusions or dislocations, and further study is needed to elucidate the nature of these defects. Origin of the revealed defects is related to deviations from stoichiometry during $ZnGeP_2$ synthesis and with growth thermal conditions, in particular, with concavity of growth interface. Rocking curves analysis confirms that crystal structure is more disturbed near the growth axis than that on periphery.

This paper reports only the initial study of structural defects for as-grown $ZnGeP_2$ crystals. In future it is planned to study the defect structure in annealed and irradiated crystals. It will also be necessary to study in future an influence of the defects, mainly the dislocations, on optical absorption in $ZnGeP_2$.

Acknowledgments

This work was supported by Siberian Branch of Russian Academy of Sciences.

References

[1] D. Creeden, P.A. Ketteridge, P.A. Budni, S.D. Setzler, Y.E. Young, J.C. McCarthy, K. Zawilski, P.G. Schunemann, T.M. Pollak, E.P. Chicklis, M. Jiang, Opt. Lett. 33 (2008) 315.
[2] Kevin T. Zawilski, Peter G. Schunemann, Scott D. Setzler, Thomas M. PollakJ. Cryst. Growth 310 (2008) 1891.
[3] D. Creeden, J.C. McCarthy, P.A. Ketteridge, P.G. Schunemann, T. Southward, J.J. Komiak, E.P. Chicklis, Opt. Express 15 (2007) 6478.
[4] D. Creeden, J.C. McCarthy, P.A. Ketteridge, T. Southward, P.G. Schunemann, J.J. Komiak, W. Dove, E.P. Chicklis, IEEE JSTQE 13 (2007) 732.
[5] N. Giles, L.E. Halliburton., MRS Bull. (1998) 37 July.
[6] S.D. Setzler, P.G. Schunemann, T.M. Pollak, M.C. Ohmer, J.T. Goldstein, F.K. Hopkins, K.T. Stevens, L.E. Halliburton, N.C. Giles, J. Appl. Phys. 86 (1999) 6677.
[7] N.C. Giles, M.M. Lihua Bai, N.Y. Chirila, K.T. Garces, P.G. Stevens, S.D. Schunemann, Setzler, T.M. Pollak, J. Appl. Phys. 93 (2003) 8975.
[8] E. Buehler, J.H. Wernick, J. Cryst. Growth 8 (1971) 324.
[9] A. Borshevskii, T. Shantsovoi, Inorg. Mater. 11 (12) (1975) 2158.
[10] A.A. Vaipolin, F.P. Kesamanli, Yu.V. Rud., Izv. Akad. Nauk SSSR, Neorg. Mater. 3 (1967) 974.
[11] K. Masumoto, S. Isomura, W. Goto., J. Phys. Chem. Solids 27 (1966) 1939.
[12] E. Buehler, J. Wernick, J. Welley, J. Electron. Mater. 2 (1973) 445.
[13] S. Fiechter, R. Castleberry, M. Angelow, K.Bachman., In: Prococeedings of the Materials Research Society, Pittsburgh, PA. Vol. 450, 1997, p. 315.
[14] G.A. Verozubova, A.I. Gribenyukov, Yu.P. Mironov, Inorg. Mater. 43 (2007) 1040.
[15] G.A. Verozubova, A.I. Gribenyukov, Crystallogr. Rep. 53 (2008) 158.
[16] R.S. Feigelson, R.K. Route, J. Cryst. Growth 49 (1980) 61.
[17] A. Authier, in: Dynamical Theory of X-Ray Diffraction, Oxford: Science Publications, 2001.
[18] G. Muller, Convection and inhomogeneities in crystal growth from melt, Crystals Growth, Properties, and Application, Springer-Verlag, Berlin, Heidelberg, 1988.
[19] L.N. Danil'chuk, A.O. Okunev, V.A. Tkal., in: X-Ray Diffraction Topography of Defects in Crystals on Base of Borrmann Effect, Yaroslav-the-Wise Novgorod State University, Veliky Novgorod, 2006.
[20] K. Sangwal, K.W. Benz, Prog. Cryst. Growth Charact. 32 (1996) 135.